

**Investigating the Release of PCBs during Dewatering  
of Ashtabula River Sediments**

**Final Report Prepared for Grant # SG 222-04**

**Sponsored by**

**Ohio Lake Erie Protection Fund**

**September 30, 2005**

**Prepared by**

**John J. Lenhart (PI)**

**Patrick J. Fox (Co-PI)**

**Department of Civil and Environmental Engineering and Geodetic Science  
The Ohio State University  
470 Hitchcock Hall, 2070 Neil Avenue  
Columbus, OH 43210**

## **Introduction**

Contaminated sediments represent a major pollution problem in the U.S. and abroad. Currently, 15 to 20 percent of National Priority List (Superfund) sites contain underwater sediment beds with metals and/or hazardous organic compounds. The U.S.-Canada International Joint Commission on the Great Lakes has identified 43 Areas of Concern (AOCs) with regard to environmental contamination. Contaminated sediments are a primary problem in 42 of these 43 AOCs. Concerns about sediment contamination in the Great Lakes region have prompted extensive study and regulatory interest (Locat et al. 2003); however many fundamental questions remain to be answered; in particular those regarding remediation of contaminated sediments in a cost-effective manner.

A typical example is the lower two-mile stretch of the Ashtabula River and Harbor, designated as an AOC in 1985 due to heavily contaminated sediments. The primary contaminants of concern include polychlorinated biphenyls (PCBs), polyaromatic hydrocarbons (PAHs), radionuclides, and heavy metals. PCBs are of paramount importance in aquatic environments due to their toxicity and propensity to bioaccumulate. Most of the Ashtabula sediments are too contaminated by PCBs for reuse or open-lake disposal, and confined disposal facilities (CDFs) are being considered for dewatering and final disposal. The Ashtabula River cleanup effort is representative of remedial actions that will be needed at similar sites in the region.

For sites like the Ashtabula River, sediment dredging and disposal is by far the most common remedial option because (1) the contaminants are removed from the environment and (2) the wide variety of contaminants in each system generally precludes the effective use of contaminant-specific cleanup methods. Dredged sediments are predominately fine-grained and have a high water content. Disposal of free liquids in a landfill is prohibited by law, and thus the sediments must be dewatered. For the Ashtabula River project, approximately one-half of the pore water contained in the dredged sediment must be removed (and treated) at an estimated cost of \$4.9M. Typically, dewatering of sediment represents one of the greatest technical challenges for a dredging and disposal remedial action.

The objective of our research was to examine the release of PCBs from Ashtabula River sediment during simulated dewatering conditions. Experiments were conducted to characterize the physical and geotechnical properties of the sediment and to determine the distribution of PCBs associated with different particle fractions of the Ashtabula River sediments. Kinetic batch experiments and simulated consolidation experiments were conducted using the bulk sediment and isolated fractions to investigate the extent and rate of PCB release that might occur

during dewatering. Our results indicate that the PCBs are concentrated in large-sized light sediment particles that comprise approximately 2 percent of the total sediment mass. Over an extended time scale and with the introduction of low PCB water, such as during dredging and passive dewatering in a CDF, these PCBs can release from the sediment particles to the pore water at a slow rate. However, over much shorter time scales, such as associated with mechanically-assisted dewatering (e.g., filter press, centrifuge), our results suggest that PCB release from the sediment particles should be minimal.

## **Materials and Methods**

### *Sediment*

The sediment used in this study was collected from the Ashtabula River just below the entrance of Fields Brook on November 19, 2004 with the assistance of personnel from Ohio EPA. Four samples were collected in 4-inch diameter Teflon-lined core tubes manually driven to a depth approximately 10 ft. below the water surface. The 10 ft. tubes, containing on average 6 ft. of sediment and 4 ft. of river water, were extracted and cut into 3 pieces (i.e., 2 sections with sediment and 1 section with river water). The ends of the tubes were sealed and the samples were transported immediately to OSU. The sections corresponding to the deepest sampling from the four cores were transferred from the core tubes under an inert nitrogen atmosphere and homogenized in a stainless steel storage container. The contents of the four river water tube sections were decanted into a clean plastic container. Both containers were stored in the dark at 4 °C.

The index properties of the Ashtabula River sediment were determined following standard ASTM methods and are shown in Table 1. The sediment is classified according to the Unified Soil Classification System as ML, being primarily comprised of inorganic silts and fine sands. The sediment average grain size was determined as 37  $\mu\text{m}$  based on sieve analysis (Appendix A). Mineralogical analysis of the sediment using x-ray diffraction indicates mainly the clay mineral illite, with smaller amounts of quartz and muscovite (Appendix A). The sediment was separated by wet sieving into three size fractions for further analyses ( $> 75 \mu\text{m}$ ,  $75 - 25 \mu\text{m}$ , and  $< 25 \mu\text{m}$ ). Light and heavy fractions of the large-sized fraction ( $> 75 \mu\text{m}$ ) were also isolated based on differences in specific gravity using a saturated calcium sulfate solution. Carbon and nitrogen contents, as determined with a Thermoquest NC 2100 analysis of the bulk and isolated sediment fractions, indicate that the large-sized light fraction, which comprised 1.8% of the total sediment mass, was primarily composed of organic matter (Table 2). The other fractions had a significant, albeit smaller, organic contents. The pore water elemental composition was determined on a water sample collected by centrifugation (Table 3). Major cations in the

sediment are Ca, Mg (not shown) and Mn, with lesser amounts of Fe and Al, and trace amounts of Cu. Significant levels of sulfur were also measured.

Table 1 - Physical/chemical properties of the Ashtabula River sediment.

Property		Value	Standard Method
Moisture Content (%)		68.7	ASTM D 2216 - 98
Atterberg Limits	Liquid Limit (%)	36.8	ASTM D 4318 - 98
	Plastic Index (%)	11.2	
Specific Gravity		2.81	ASTM D 5550 - 94
Grain Size Distribution	Mean Grain Size ( $\mu\text{m}$ )	37	ASTM D 422 - 63

Table 2 - Carbon and nitrogen content (% dry weight).

Description		Nitrogen	Carbon
Bulk Sediment		0.14	3.24
Particle Size	> 75 $\mu\text{m}$	0.29	8.23
	75 - 25 $\mu\text{m}$	0.12	1.69
	< 25 $\mu\text{m}$	0.17	1.98
Density	Light	1.02	28.35
	Dense	0.00	1.44

Table 3 - Elemental composition of sediment pore water.

Species	Al	As	Ca	Cd	Co	Cr	Cu	Fe
Concentration (mg/L)	0.041	NA	610	NA	0.003	NA	0.026	0.607
Species	Mn	Mo	Ni	P	S	Se	Zn	
Concentration (mg/L)	3.06	0.007	0.015	0.049	448	NA	NA	

#### *PCB Determination*

In general, the protocols for analyzing the PCB content of water, sediment and resin samples followed EPA methods from SW-846. The PCB content in water samples was determined based on liquid-liquid extraction following EPA Method 3520C modified for small sample volumes. Extractions were performed by adding 3 mL of hexane and 25 mL of water to a sample vial that was vigorously mixed for two minutes. After shaking, the phases were allowed

to separate before the hexane was extracted. The extraction procedure was then repeated a second time and nitrogen blowdown was used to reduce the total extract volume to 1mL. PCBs were extracted from sediment samples using an automated Soxhlet extractor after Method 3541 with a 1:1 mixture of hexane and acetone. Extracts were reduced to 1mL with nitrogen blowdown prior to cleanup. Resin samples were extracted using a procedure outlined by Ghosh et al. (1999). Ten mL of a 1:1 hexane-acetone mixture were added to the sample in a 25mL vial, and placed on a rotary shaker for 24 hours. The resin was then allowed to settle before the solvent mixture was extracted. This procedure was repeated twice, before nitrogen blowdown was used to reduce the total extract volume to 1mL. Where required, cleanup was performed by passing the extracts through a 1 gram Florisil cartridge in accordance with EPA Method 3620B. PCB concentrations were determined on a HP 6890+ gas chromatograph with an electron capture detector in accordance with EPA Method 8082 and are reported for the sediment on a dry-weight basis.

#### *Kinetic batch tests*

The rate and extent of PCB desorption from the bulk and isolated fractions were determined batch-wise using the approach of Cornelissen et al. (1997). For the bulk sediment, size-fractionated isolates, and large-sized dense fraction sample tubes were filled with 1g sample (air-dried), 1g XAD-resin and 10mL of river water. For the large-sized light fraction, the sample tubes were filled with 0.2g sample (air-dried), 1g XAD-resin, and 10 mL river water. The tubes were sacrificed for PCB determination of the resin, pore water and sediment at elapsed time periods of 6hr, 1day, 3day, 5day, 1week, 2week, 3week, 4week, 5week, 6week, and 7week. At each sampling time, the resin was manually separated after increasing the density of water using a saturated solution of calcium sulfate followed by centrifugation.

#### *Consolidation tests*

Consolidation tests were performed to obtain compressibility (i.e., void ratio vs. effective stress) and hydraulic conductivity (i.e., hydraulic conductivity vs. void ratio) constitutive relationships that are required for numerical simulations of sediment dewatering. The sediment was placed in a rigid confining cell and consolidated by incremental loading using dead weights hung from a lightweight hanger system. The hanger is positioned on a piston that transfers the load through a load plate and porous disk to the specimen (Figure A.3). Hydraulic conductivity measurements were conducted at the end of each load increment using a syringe flow pump connected to the base of the consolidation test cell.

### Soil column tests

Input parameters for the numerical simulations include the effective diffusion coefficient ( $D^*$ ), dispersivity ( $\alpha$ ) and retardation factor ( $R_d$ ). A series of dispersion and diffusion column tests were conducted to determine  $D^*$ ,  $\alpha$ , and  $R_d$  for select PCB congeners, a reactive dissolved solute (potassium) and a nonreactive dissolved solute (bromide). Results from the experiments were analyzed by fitting analytical solutions. Dispersion column test results were back-calculated with following analytical solution (van Genuchten and Parker, 1984; Shackelford and Redmond, 1995),

$$c_e(L, t) = \frac{c_o}{2} [\text{erfc}(\xi_1) + \exp(\xi_2) \text{erfc}(\xi_3)] \quad (1)$$

where  $c_e$  is the effluent concentration,  $c_o$  is the reservoir concentration,  $\text{erfc}$  is the complementary error function, and the dimensionless arguments are defined as,

$$\xi_1 = \frac{1 - T_R}{2\sqrt{\frac{T_R}{P_L}}}; \quad \xi_2 = P_L; \quad \xi_3 = \frac{1 + T_R}{2\sqrt{\frac{T_R}{P_L}}}; \quad T_R = \frac{\nu t}{R_d L}; \quad P_L = \frac{\nu L}{D} \quad (2)$$

where  $\nu$  is the seepage velocity,  $L$  is the specimen length,  $D$  is the hydrodynamic dispersion coefficient ( $D^* + \alpha\nu$ ), and  $P_L$  is the Peclet number. The analytical solution for the diffusion test is (Shackelford and Daniel, 1991),

$$\frac{c_t}{c_o} = \frac{\alpha}{1 + \alpha} + \sum_{m=1}^{\infty} \frac{2\alpha}{1 + \alpha + \alpha^2 q_m^2} \exp\left(\frac{-D^* q_m^2 t}{R_d L^2}\right) \quad (3)$$

where  $c_t$  is the concentration of a given solute in the reservoir at any time  $t$  after the start of diffusion. The nonzero positive root,  $q_m$ , is given by

$$\tan(q_m) = -\alpha q_m \quad (4)$$

where the dimensionless coefficient  $\alpha$  is defined as a function of the volumetric water content,  $\theta$ , and the height of the reservoir above the sediment,  $L_r$ ,

$$\alpha = \frac{L_r}{\theta R_d L} \quad (5)$$

A schematic diagram of the dispersion column test is shown in Fig. A.4. For this test, the specimen was placed in the column by a combination of spooning and careful tapping to remove entrapped air bubbles. A syringe flow pump was connected to the base of the column to provide upward water flow upward through the specimen. The magnitude of flow was determined to minimize seepage consolidation during the test. The sediment soil specimen was 5 cm in height and the seepage velocity was  $27.6 \times 10^{-6}$  cm/sec. Reservoir concentrations were 404 and 838 ppm for  $K^+$  and  $Br^-$ , respectively. Each water sample was removed for analyses at a predetermined time increment corresponding to a flow of 0.25 pore volume. Concentrations of bromide and potassium were measured using ion-selective electrodes connected to a combination mV/pH meter.

The diffusion column tests were performed to determine values of  $D^*$  for the Ashtabula River sediment. Sediment was placed in the diffusion column to a height of 15 cm and then water from a Millipore water system (Milli-Q water) was placed over the specimen to a depth of 7 cm (Fig. A.5). The column was sealed and stored for 2 weeks to ensure equilibrium with regard to shrink/swell. The Milli-Q water was then carefully removed using a pipette and an identical volume of Milli-Q water supplemented with 408 and 800 mg/L potassium (as KCl) and bromide (as NaBr), respectively, was added to the column.  $K^+$  and  $Br^-$  concentrations in the reservoir were monitored using ion-selective electrodes carefully inserted into reservoir. Prior to each measurement, the solution reservoir was stirred to achieve uniform concentration.

#### *Dewatering test*

Dewatering of Ashtabula River sediment was studied experimentally using a modified one-dimensional consolidation test. The dewatering test apparatus (Fig. A.6) is similar to the previously-described consolidation test apparatus; however, instead of connecting a flow pump to the base for hydraulic conductivity measurements, a peristaltic pump was used to collect effluent water samples from the reservoir above the porous stainless steel disk throughout the duration of the test. One dewatering test was conducted using a sediment specimen that was at the same initial water content as in the riverbed (68.7%). Incremental loads were placed on the specimen equal to 2.8, 7.5, 16.7, 35.2, and 72.3 kPa. The first load remained on the specimen for 48 hours and each subsequent increment remained on the specimen for 24 hours. The effluent was collected using the peristaltic pump and analyzed for PCB. At the conclusion of the test, the sediment sample was extruded from the apparatus and dissected into eight equal-

sized fractions that were analyzed to determine the final PCB concentration profile.

## Results and Discussion

### *PCB content*

Initial testing of the bulk sediment identified 74 peaks representing 104 different PCB congeners in the sediment. Several prevalent peaks were selected for further study. These include peaks corresponding to PCBs 5/8, 28/31, 52, and 66/95. Concentrations of these congeners varied widely between samples, with average values given in Table 4.

Table 4 - Concentrations of Selected PCB Congeners in the Bulk Sediment

IUPAC #	PCB Structure	Concentration ( $\mu\text{g}/\text{kg}^*$ )
PCB 5/8	2,3-DiCB and 2,4'-DiCB	1000 $\pm$ 500
PCB 28/31	2,4,4'-TriCB and 2,4',5-TriCB	400 $\pm$ 300
PCB 52	2,2',5,5'-TetraCB	1000 $\pm$ 700
PCB 66/95	2,3',4,4'-TetraCB and 2,2',3,5',6-PentaCB	500 $\pm$ 500

\*1 $\mu\text{g}/\text{kg}$  = 1 ppb

After the sediment was separated into four fractions based on size and density, the individual fractions were analyzed for PCB content. The large-sized, light material, which is mostly organic, contains the highest levels of each PCB (see Table 5). The large-sized dense fraction still contains significant amounts of PCBs, although at an order of magnitude less than the light, organic fraction. The small-sized fractions contain trace amounts of PCBs, near or below the

Table 5. Concentration of Selected PCB Congeners in Various Sediment Fractions

PCB	Concentration ( $\mu\text{g}/\text{kg}$ )				
	<25 $\mu\text{m}^*$	25 $\mu\text{m}$ -75 $\mu\text{m}^*$	>75 $\mu\text{m}$ Light <sup>@</sup>	>75 $\mu\text{m}$ Dense*	Total <sup>&amp;</sup>
5/8	10	10	16000	10	300
28/31	10	BD	1000	300	60
52	BD	BD	4000	900	200
66/95	20	40	200	100	47

BD: Below method detection level

\*Based on the analyses of one sample

@Based on the analyses of nine samples

&Total = (0.38)small-sized + (0.48)medium-sized + (0.018)large-sized light + (0.122)large-sized dense

detection limit. The total PCB content in the sediment based upon summing the weight-normalized isolate concentrations was below that determined for the bulk sediment by on average a factor of six, further emphasizing the heterogeneous distribution of PCBs within the sediment. We intend to continue to work on refining our procedures to quantify PCBs in both the bulk sediment and the isolated sediment fractions.

#### *Batch Tests*

Pore water and resin samples from nearly all of the kinetic batch test experiments contained trace amounts of PCB at or below the detection limit. The results collected for the release of PCBs from the large-sized light sediment being the one exception. Results indicate that the extent and rate of release is gradual for PCB congeners 5/8, 28/31 and 52, whereas for PCBs 66/95 release occurs more quickly and to a greater extent (Figure 1). In each case, the rates appear to exhibit an initial rapid release stage during the first several days, followed by a second much slower release stage that continued until the final sample was sacrificed. The results also suggest for the time period studied that the PCBs were strongly bound to the large-sized light sediment particles as the extent of release remained below 10 percent except for PCBs 66/95.

Measured constitutive relationships are shown in Fig. 2(a) and 2(b). As effective stress increases from 2.8 to 72.3 kPa, the void ratio decreases from 1.59 to 1.14 and the hydraulic conductivity decreases from  $1.31 \times 10^{-8}$  to  $2.10 \times 10^{-9}$  m/sec. Fig. 3(a) shows dispersion test results and best-fit analytical solution curves for potassium and bromide in the bulk sediment. Estimated hydrodynamic dispersion coefficients for potassium and bromide in the sediment are 16.90 and  $21.8 \times 10^{-6}$  cm<sup>2</sup>/sec, respectively. The contaminant distribution coefficients for this test were determined to be zero for bromide (indicating no interaction) and 2.33 mL/g for potassium. Fig. 3(b) shows experimental diffusion test results and best-fit model curves. The effective diffusion coefficients for potassium and bromide are  $5.25 \times 10^{-6}$  and  $5.24 \times 10^{-6}$  cm<sup>2</sup>/sec, respectively. From these tests, we calculated dispersivities of 0.42 and 0.58 cm for potassium and bromide, respectively. Based on diffusion coefficients for potassium and bromide in free solution ( $19.6$  and  $20.8 \times 10^{-6}$  cm<sup>2</sup>/sec respectively; Shackelford, 1988), estimated tortuosities are 0.27 and 0.25. The water samples collected from the consolidation experiments, as well as the final sediment specimen slices, were of insufficient size to accurately measure PCBs, with all measurements at or below the detection limit.

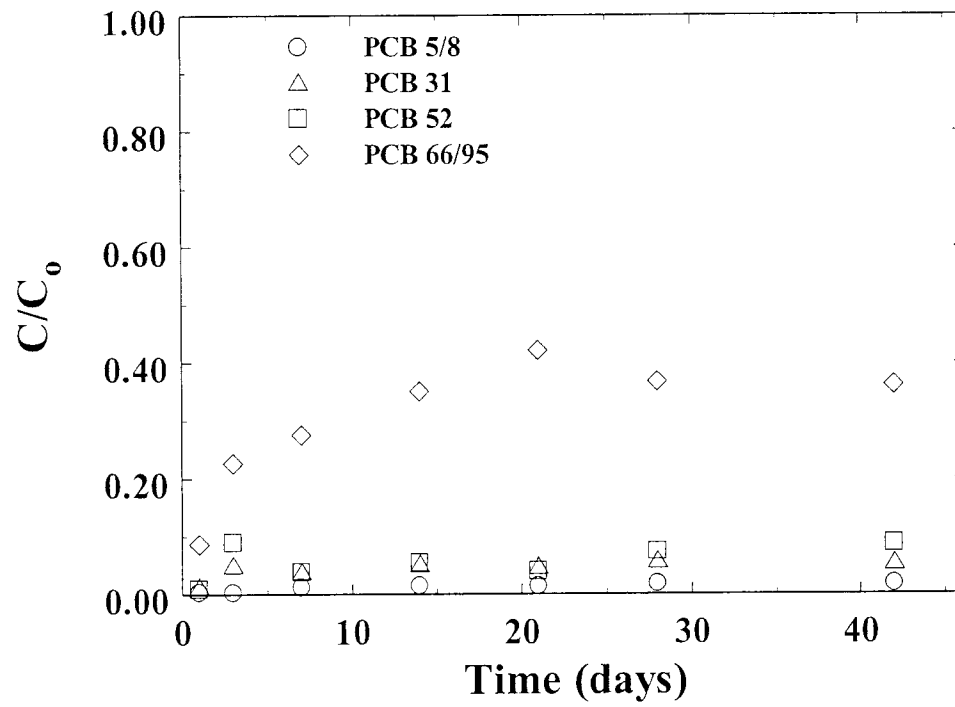
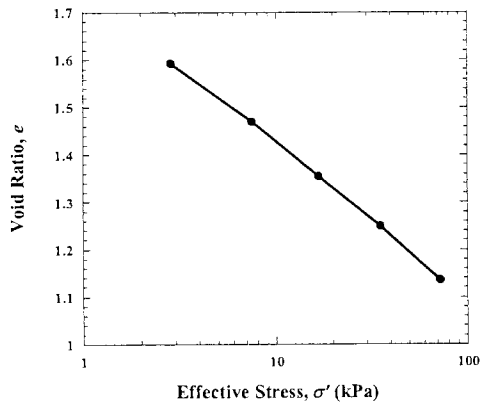
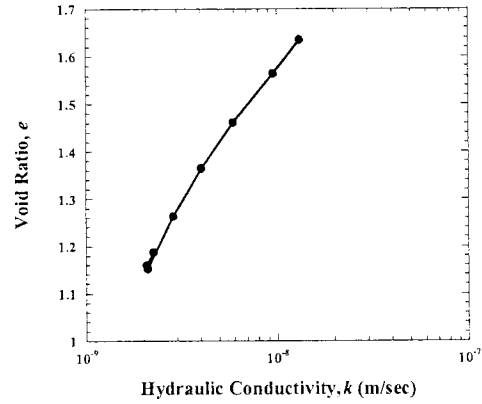


Figure 1. PCB release in the organic fraction of the sediment.

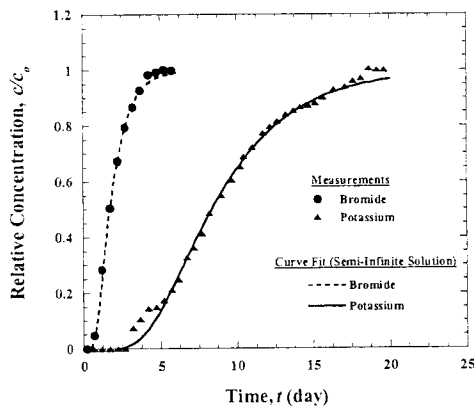


(a)

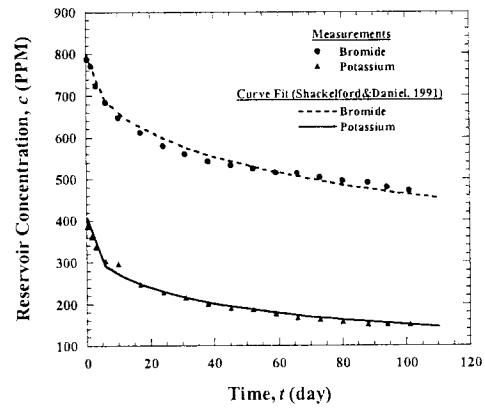


(b)

Fig. 2. Constitutive relationships for Ashtabula River sediment: (a) Void ratio vs. effective stress and (b) Hydraulic conductivity vs. void ratio.



(a)



(b)

Fig. 3. Experimental results and best-fit model curves for potassium and bromide in the bulk sediment: (a) Dispersion test results and (b) Diffusion test results.

Results of the dewatering test were simulated using the numerical model CST1 (Fox 2005a, 2005b) with the independently measured input parameters (Table 1) and constitutive relationships (Figure 2). The overall comparison is shown in Figure 4 and the comparisons for the five individual load increments are shown in Appendix B. In general, the CST1 model predictions are in excellent agreement with the measured values. The final average moisture content of the sediment specimen was 40.6% (down from an initial value of 68.7%).

Consolidation-induced PCB transport was simulated for Ashtabula River sediment that is placed in a confined disposal facility (CDF). The bottom of the CDF is assumed to be lined, and a saturated slurry layer is placed relatively quickly to an initial height of 7 m and then consolidates by self-weight. Material properties are based on the above test results. The slurry has  $G_s = 2.81$  and an initial void ratio of 1.93. It is assumed that the layer remains saturated and that the upper water level is coincident with the top boundary. Other contaminant migration pathways, such as plant or animal uptake and airborne emissions, and other physical effects such as surface desiccation are not considered in this example. These effects may be important for the performance of an actual CDF. Fig. 5 shows settlement vs. time for the single-drained case (drainage only through the top of the sediment layer). Final settlement is 1.36 m, 96% of which occurs in 5 years. The mass of PCBs released can be estimated assuming the pore water expelled during dewatering is in equilibrium with the PCB-contaminated sediments. For example, based on an estimated sediment organic matter fraction of 0.065 (calculated from twice the carbon content of 0.0324; Table 2), we estimate a value for the partition coefficient ( $K_d$ ) for PCB 52 of 10,000. For a uniform initial PCB concentration of 1000  $\mu\text{g}/\text{kg}$  (Table 4) this gives a pore water concentration at equilibrium of approximately 100 ng/L. Thus, approximately 140 mg of PCB 52 is estimated to be released over a 5 year period for every square meter of consolidating sediment.

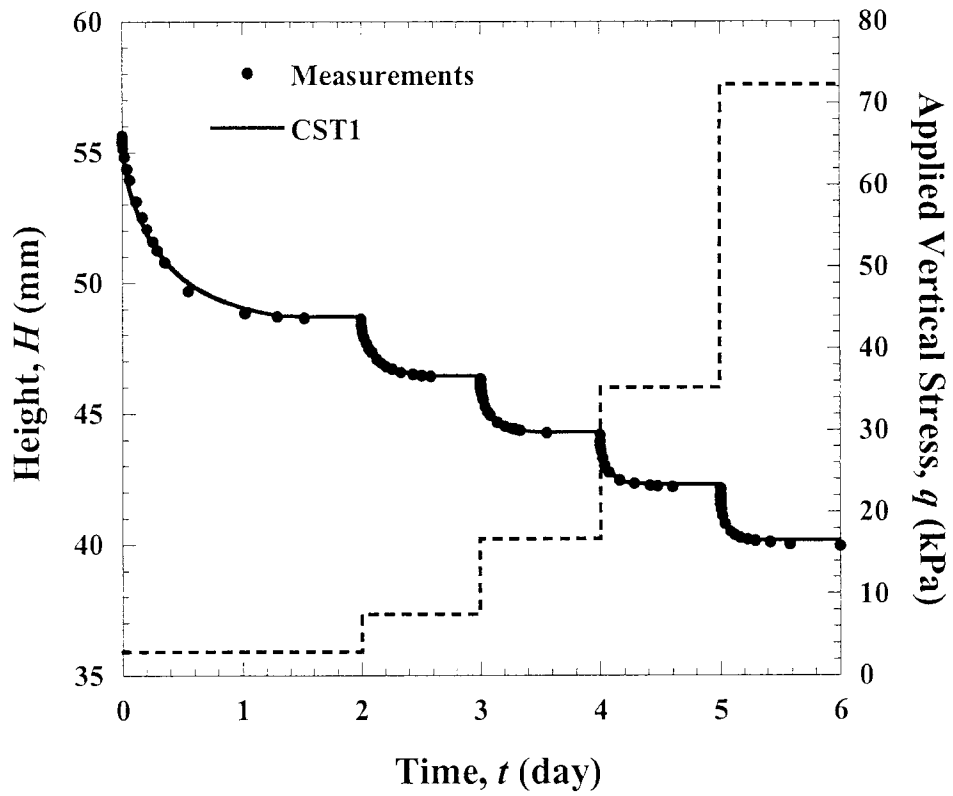


Fig. 4. Comparison between measured sediment specimen height and numerical predictions for dewatering test.

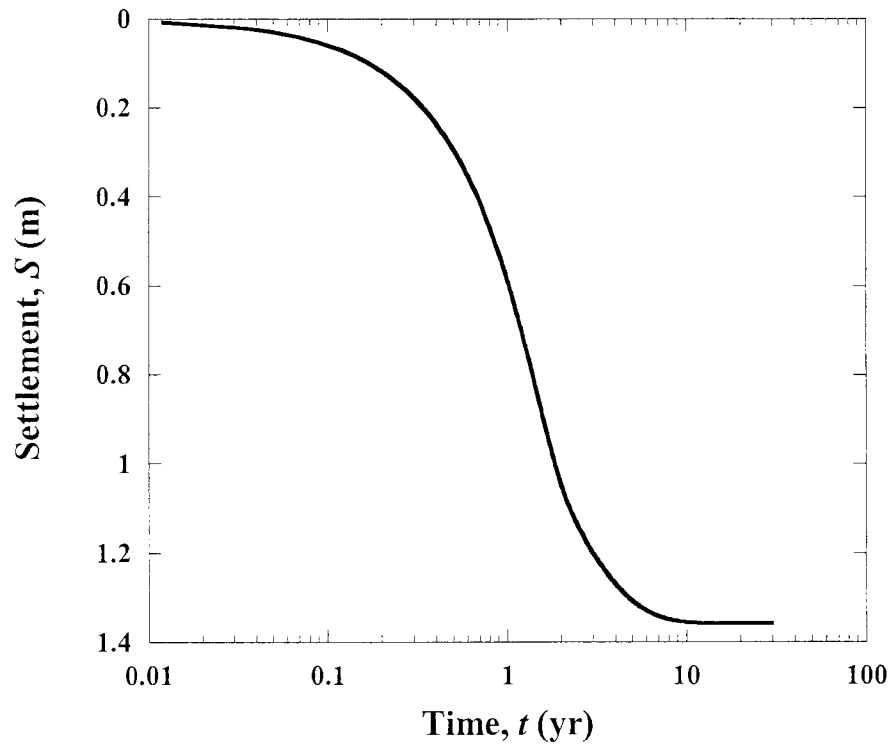


Fig. 5. Predicted settlement vs. time relationship for single-drained condition in a CDF.

## Summary and Conclusion

Based on the analyses of sediment fractions isolated as a function of size and density, the majority of the PCBs within the Ashtabula River sediments are concentrated in large sized, light material that is primarily organic in content. This sediment fraction appears to strongly bind PCBs, thus minimizing their release to uncontaminated water as the rate and extent of release over the time period examined for all but one of the congeners studied was low. It is likely that a remedial technique designed to exploit particle density differences within the sediment (i.e., separating the sediment into density fractions) could significantly reduce the PCB load of the sediment.

Predictions using the numerical model CST1 closely matched experimental data for sediment consolidation under applied load. Although PCB release during these experiments was too low to measure, additional work examining contaminant release from laboratory-synthesized sediment (data not shown in this report) indicates the model can accurately simulate consolidation-induced contaminant transport, such as would occur within a sediment confined disposal facility (CDF). Simulating the self-weight consolidation of the Ashtabula River sediment impounded in a CDF suggests that a significant reduction in water content will take years and that significant amounts of PCBs could be released during the dewatering process.

Future work examining the release of PCBs from sediments over longer time periods and under loading regimes similar to those observed in a CDF or during *in situ* consolidation is needed to verify the model's predictability. It is also important to examine how colloid-sized particles act to facilitate or hinder the migration of sparingly-soluble contaminants such as PCBs during various remedial scenarios, particularly as the majority of the PCBs and presumably other organic contaminants are associated with low-density organic particles that would presumably be mobilized more readily than would the heavier mineral particles.

## References

- Cornelissen, G., van Noort, P. C. M., Parsons, J. R. and Govers, H. A. J. (1997). "Temperature dependence of slow adsorption and desorption kinetics of organic compounds in sediments." *Environmental Science and Technology* **31**(2): 454-460.
- Fox, P. J. (2005a), "Coupled large strain consolidation and solute transport. I: Model development," *Journal of Geotechnical and Geoenvironmental Engineering*, accepted for publication.
- Fox, P. J. (2005b), "Coupled large strain consolidation and solute transport. II: Model verification and simulation results," *Journal of Geotechnical and Geoenvironmental Engineering*, accepted for publication.
- Ghosh, U., Weber, A. S., Jensen, J. N. and Smith, J. R. (1999). "Congener level PCB desorption kinetics of field-contaminated sediments." *Journal of Soil Contamination* **8**(5): 593-613.
- Locat, J., Galvez-Cloutier, R., Chaney, R., and Demars, K., eds. (2003). "Contaminated Sediments: Characterization, Evaluation, Mitigation, Restoration, and Management Strategy Performance," STP 1442, American Society for Testing and Materials.
- Shackelford, C. D. and Redmond, P. L. (1995), "Solute breakthrough curves for processed kaolin at low flow rates," *Journal of Geotechnical Engineering*, **121**(1): 17-32.
- Shackelford, C. D. and Daniel, D. E. (1991), "Diffusion in saturated soil. II: Results for compacted clay," *Journal of Geotechnical Engineering*, **117**(3): 485-506.
- Shackelford, C. D. (1988), "Diffusion of inorganic chemical wastes in compacted clay," thesis presented to the University of Texas, at Austin, Tex., in partial fulfillment of the requirements for the degree of Doctor of Philosophy.
- van Genuchten, M. T. and Parker, J. C. (1984), "Boundary conditions for displacement experiments through short laboratory soil columns," *Soil Science Society of America Journal*, **48**: 703-708.

Appendix A : Sediment particle size distribution and mineralogy analyses, and schematic diagrams of experimental testing program.

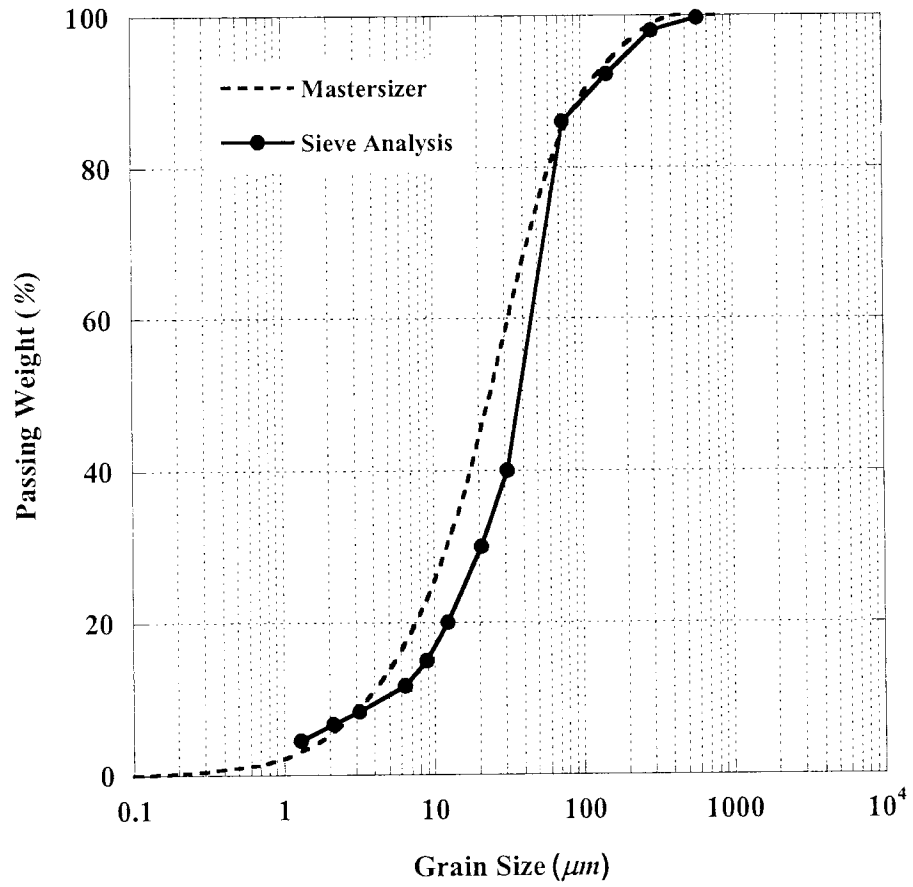


Fig. A.1. Particle size distribution by sieving and a Malvern Instruments Mastersizer.



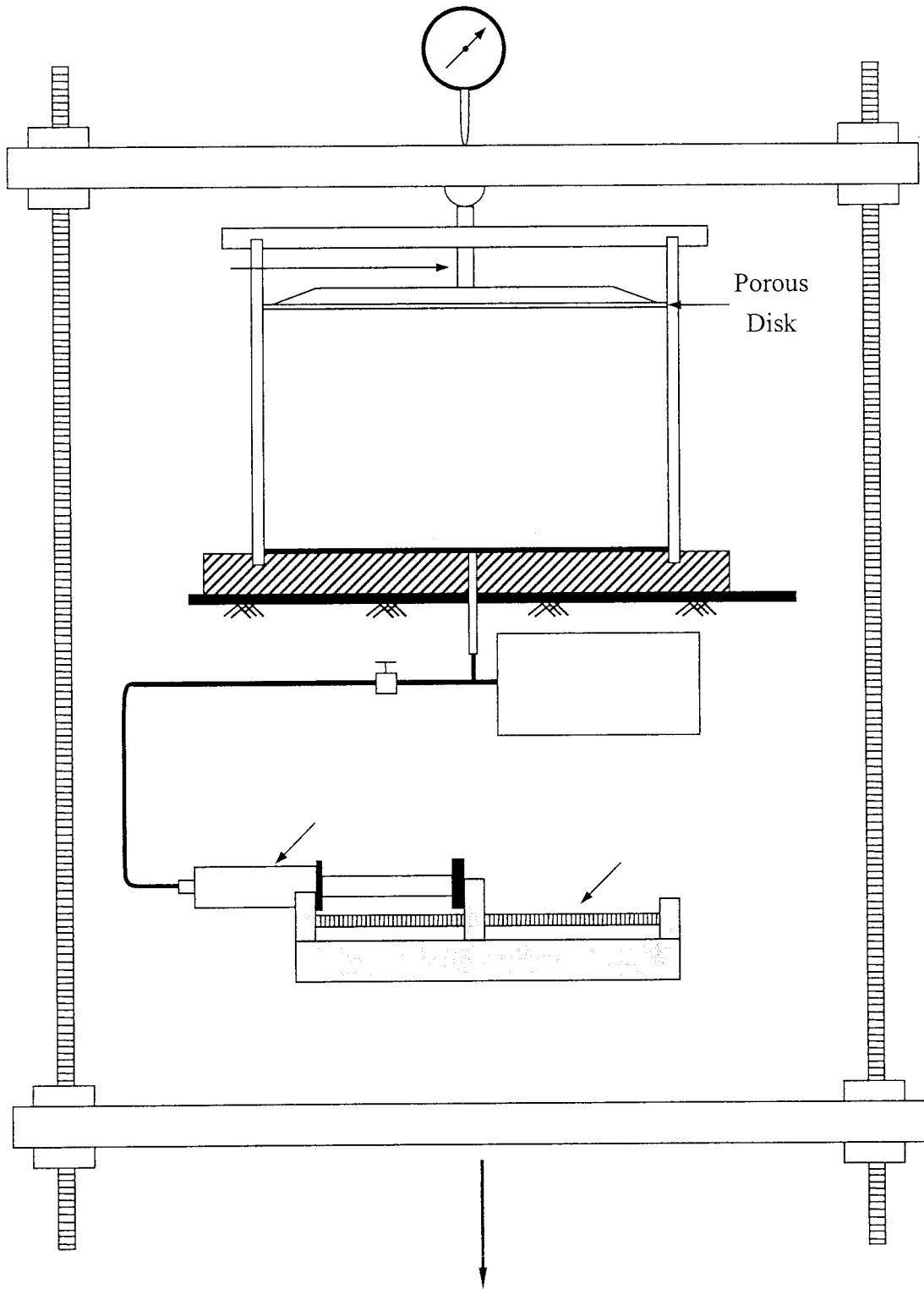


Fig. A.3. Schematic diagram of consolidation test apparatus.

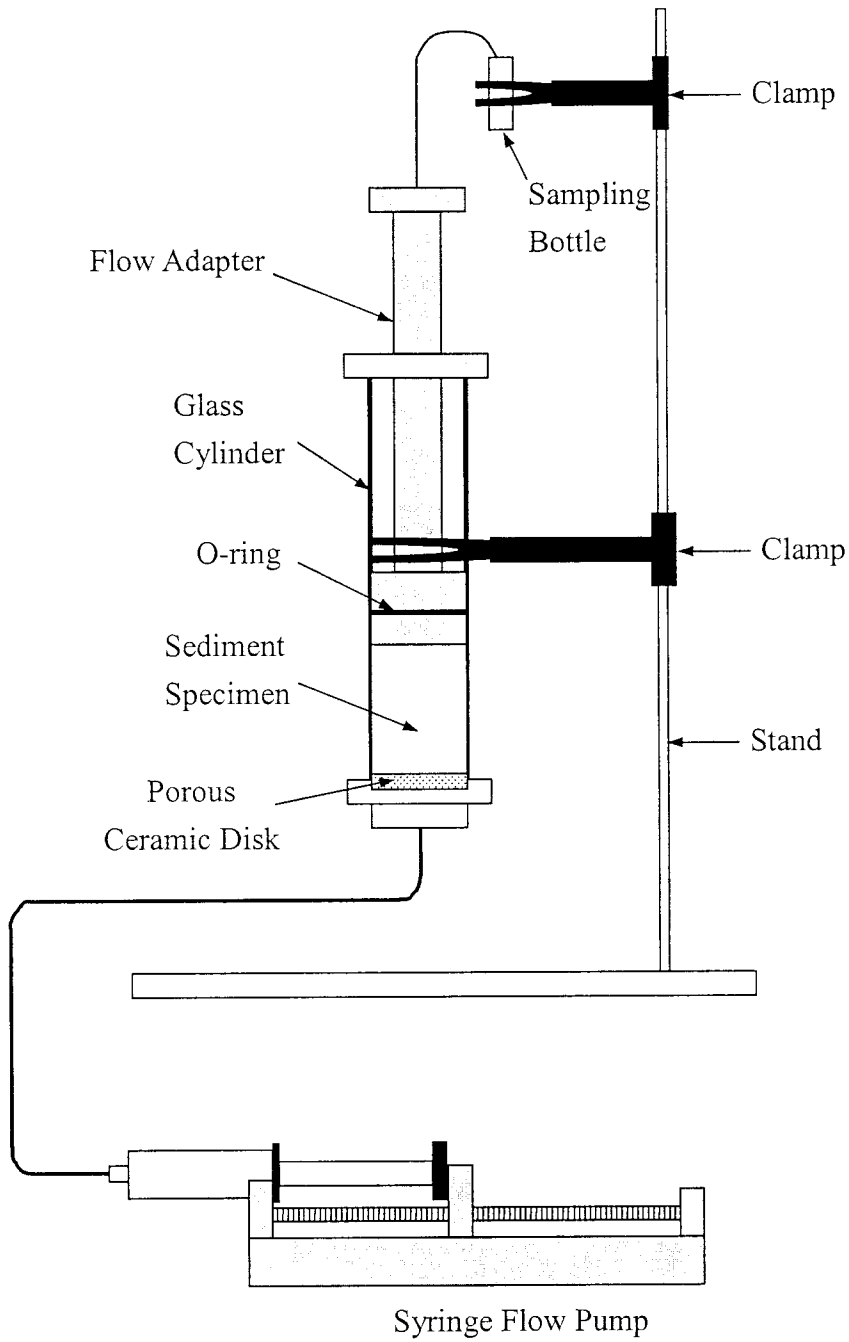


Fig. A.4. Schematic diagram of dispersion test apparatus.

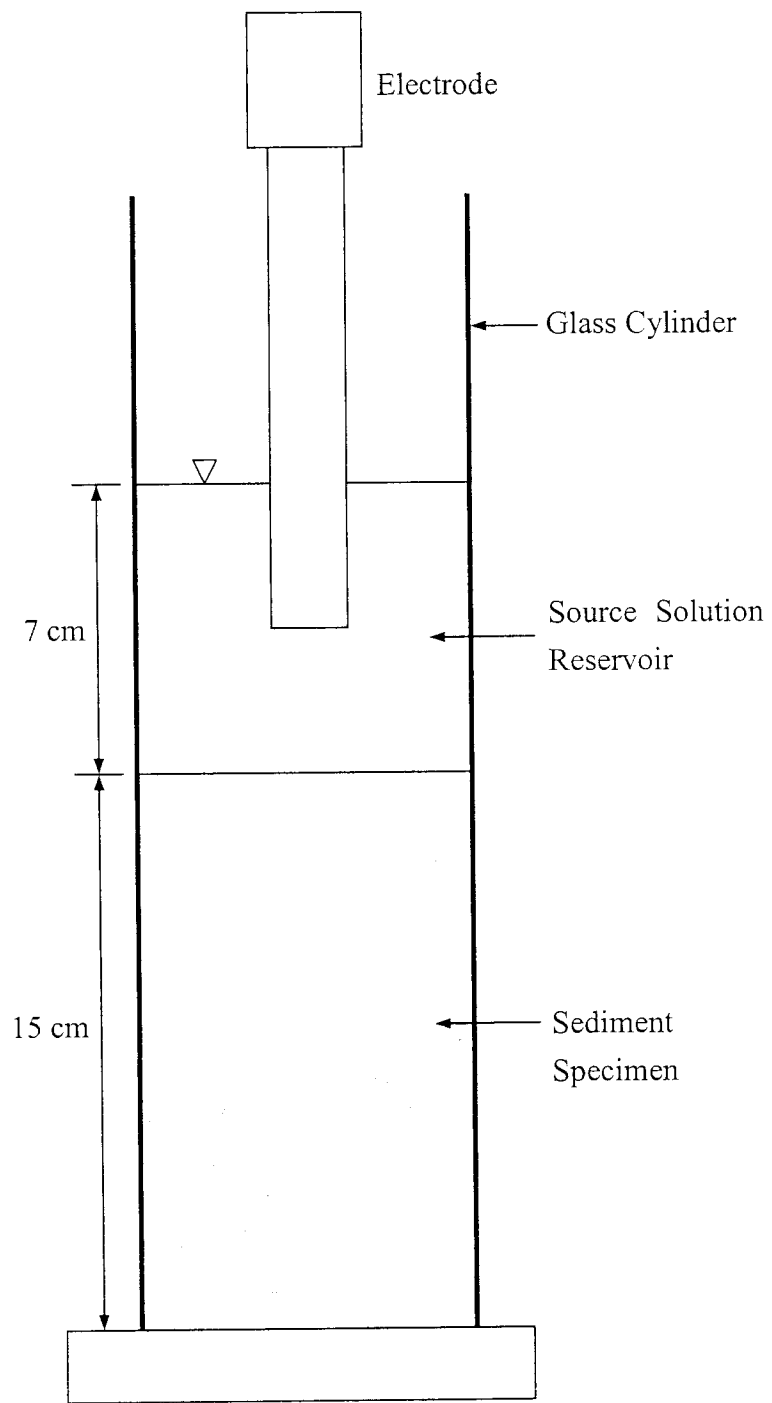


Fig. A.5. Schematic diagram of diffusion test apparatus.

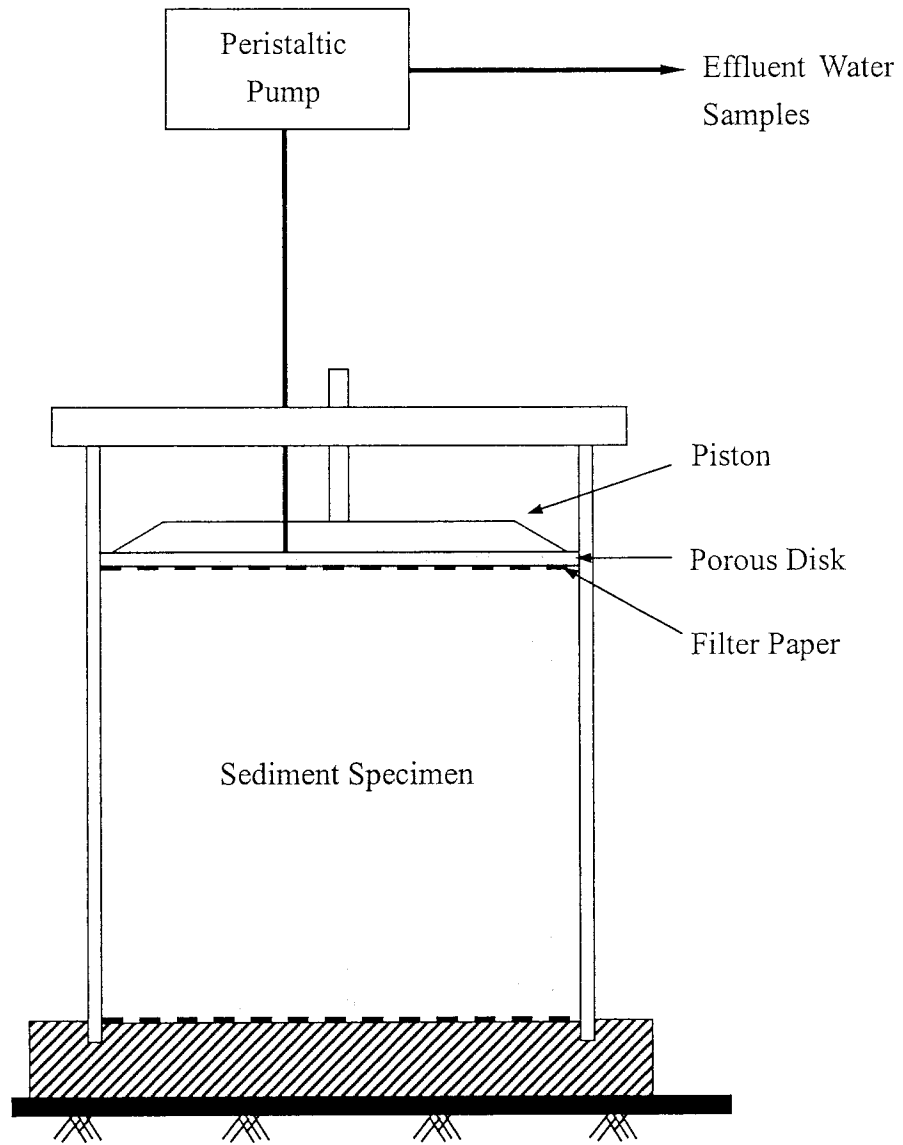


Fig. A.6. Schematic diagram of dewatering test apparatus.

Appendix B : Dewatering test results and numerical simulation

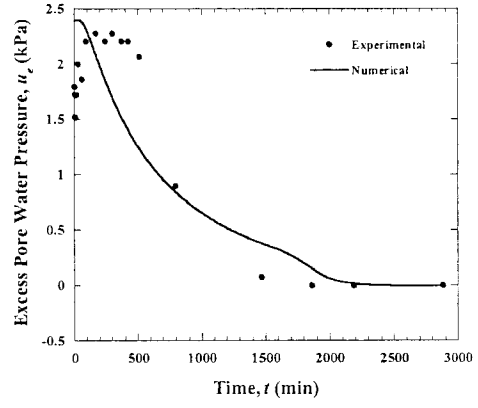
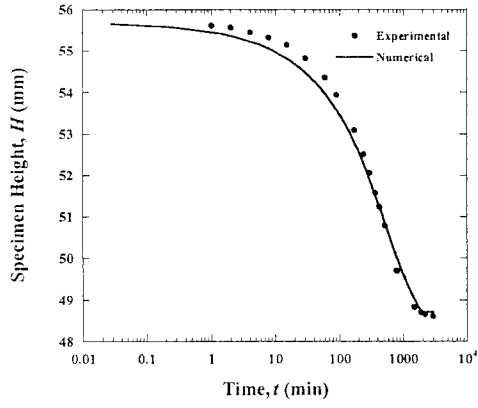


Fig B.1. Load increment 1

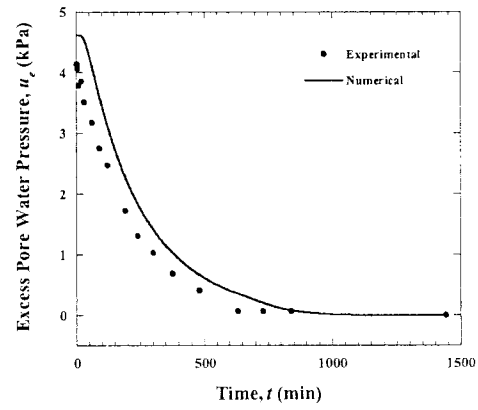
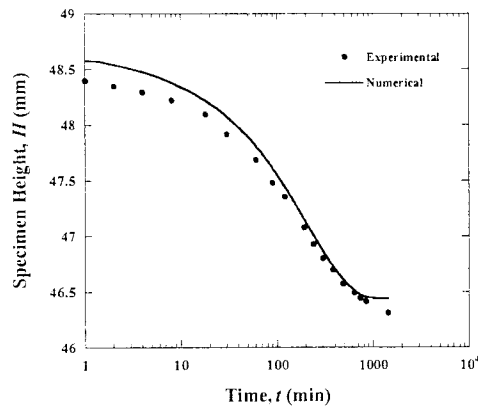


Fig. B.2. Load increment 2

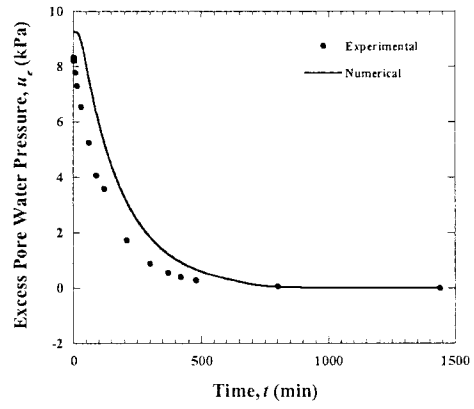
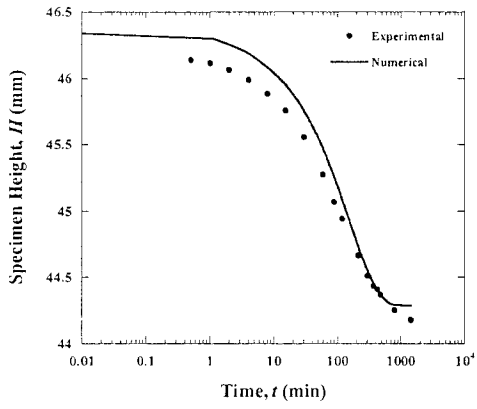


Fig B.3. Load increment 3

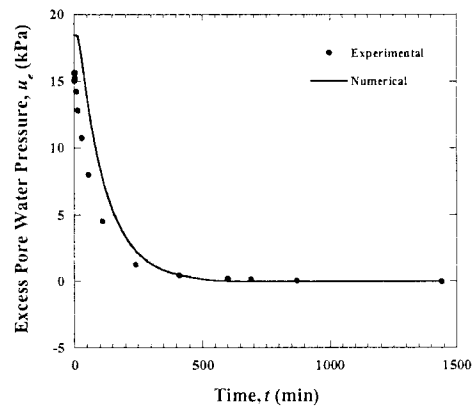
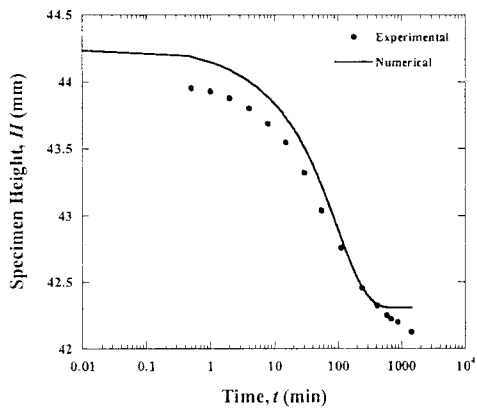


Fig. B.4. Load increment 4

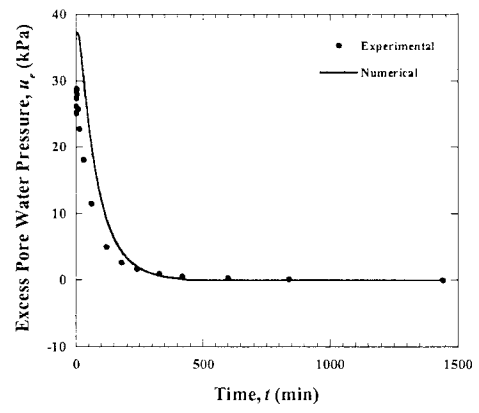
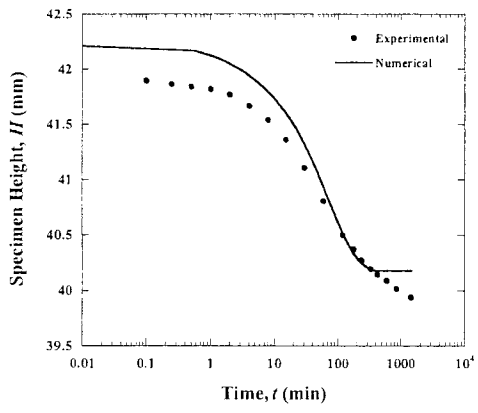


Fig B.5. Load increment 5